



## The limits to northern peatland carbon stocks

Georgii A. Alexandrov<sup>1</sup>, Victor A. Brovkin<sup>2</sup>, Thomas Kleinen<sup>2</sup>, Zicheng Yu<sup>3,4</sup>

<sup>1</sup> A.M. Obukhov Institute of Atmospheric Physics, Russian Academy of Sciences, Pyzhevsky 3, Moscow, 119017, Russia

<sup>2</sup> Max Planck Institute for Meteorology, Bundesstrasse 53, 20146 Hamburg, Germany

5 <sup>3</sup>Department of Earth and Environmental Sciences, Lehigh University, 1 West Packer Avenue, Bethlehem, PA 18015, USA

<sup>4</sup>Institute for Peat and Mire Research, School of Geographical Sciences, Northeast Normal University, Changchun 130024, China

*Correspondence to:* Victor A Brovkin ([victor.brovkin@mpimet.mpg.de](mailto:victor.brovkin@mpimet.mpg.de))

10 **Abstract.** Northern peatlands have been a persistent natural carbon sink since the last glacial maximum. If there were no limits to their growth, carbon accumulation in these ecosystems could offset a large portion of anthropogenic carbon emissions until the end of the present interglacial period. Evaluation of the limits to northern peatland carbon stocks show that northern peatlands will potentially play an important role, second only to the oceans, in reducing the atmospheric carbon dioxide concentration to the level that is typical of interglacial periods if cumulative anthropogenic carbon emissions will be  
15 kept below 1000 Pg of carbon.

### 1 Introduction

The recent compilations of peatland data (Loisel et al., 2014) largely confirm the conventional wisdom of the carbon (C) sink provided by northern peatlands since the Last Glacial Maximum (Loisel et al., 2017). According to this notion, northern peatlands were providing a persistent but variable sink for atmospheric carbon (Yu, 2011). The variations are explained by  
20 changes in the rate of peatland expansion and in the rate of peat accumulation. In the early Holocene, both the rate of peatland expansion and the rate of carbon accumulation appear to be highest (Yu et al., 2010) as compared to the later periods. However, during the last 5000 years, the area of peatlands remained relatively stable (Adams and Faure, 1998), and therefore the growth in peat depth could be the major cause of the carbon sink provided by northern peatlands.

The average rate of carbon accumulation associated with peat growth is estimated at 18–28 gC m<sup>-2</sup> yr<sup>-1</sup> (Yu, 2011). This rate  
25 suggests that northern peatlands, occupying 2.4–4 million km<sup>2</sup> (Yu, 2011), may accumulate 864–2240 PgC during the next 20,000 years—that is, an amount of carbon that is comparable to the expected cumulative anthropogenic carbon emissions corresponding to a 2.5°C warming (Raupach et al., 2014).

There is, of course, no guarantee that the current interglacial will last for another 20,000 years; however, the recent attempts to estimate its possible duration lead to conclusion that a glacial inception is unlikely to happen within the next 50,000 years  
30 if cumulative carbon emissions exceed 1000 PgC (Berger et al., 2016). Since the duration of the current interglacial depends



on the cumulative carbon emissions, it should also depend on the cumulative carbon removal that may offset the effect of carbon emissions.

There has been little research, however, on estimating the potential magnitude of the cumulative carbon removal associated with the natural development of peatland ecosystems. Individual peatland development may lead to reduction of the carbon sink potential: the closer the peatland ecosystem is to its steady state, the lower is the carbon sink magnitude. Therefore, the amount of carbon that northern peatlands could remove from the atmosphere might be less than that estimated above.

The process of reaching equilibrium could be conceptualized as follows. Peat is accumulated due to protection of plant litters in the catotelm, the lower layer of a peat deposit that is permanently saturated with water. The plant litters do not enter the catotelm directly, but instead they first enter to the upper layer of the peat deposit, the so-called acrotelm, that is not permanently saturated with water. Despite intense aerobic decomposition of organic matter in the acrotelm, at least a small portion of the organic matter that enters the acrotelm always reaches the catotelm in an accumulating peatland.

Precisely speaking, the organic matter does not reach the catotelm, it is rather “flooded” by elevating groundwater. The elevation of groundwater is caused by the elevation of the peatland surface that in turn results from accumulation of organic matter. This loop cannot elevate the groundwater infinitely. The maximum height of the water table, and thus the potential peat depth, is determined by the amount of effective rainfall, drainage system density and the hydraulic conductivity of peat and mineral materials below the peat.

To calculate the potential peat depth, we apply an equation (see *Methods*) derived from the impeded drainage model used in our previous study (Alexandrov et al., 2016). This equation relates the maximum peat depth at a given watershed to the fraction of its area covered by peatland and the average depth to bedrock, and thus allows us to estimate the potential amount of carbon that could be accumulated in northern peatlands from gridded data of soil properties (Batjes, 2016) and depth to bedrock (Hengl et al., 2014).

The gridded data on soil properties give the fraction of a grid cell covered by peatlands. To estimate the fraction of a watershed covered by peatlands, which is needed for calculating the potential peat depth, one should make an assumption about the peatland distribution within the grid cell. We address the uncertainty associated with making such assumptions by giving three estimates of the potential amount of carbon that could be accumulated in northern peatlands: conservative estimate, non-conservative estimate and less-conservative estimate. The conservative estimate assumes uniform distribution of peatlands over all grid cells, the non-conservative estimate assumes clustered distribution over all grid cells, and the less-conservative estimate is derived using a rule-based algorithm categorizing the grid cells into those where peatland distribution is uniform and those where peatland distribution is clustered (see *Methods*).



## 2 Methods

The maximum depth of peat that could be accumulated in a watershed is a function of effective rainfall (the difference between precipitation and evapotranspiration), the density of draining system, and the average height of the watershed above the level of draining system. The particular form of this function, derived by using the impeded drainage model (IDM) approach, implies that the maximum carbon stock in a grid cell,  $p_{C,max}$ , can be estimated using the following equations:

$$\begin{cases} p_{C,max} = c \times A \times \left( (h_{max} - g) - \frac{1}{3} \left( h_{max} - g \left( \frac{g}{h_{max}} \right)^2 \right) + d \times f_{P,obs} \right) \\ h_{max} = \frac{g}{\sqrt{1-f_{P,obs}}} \end{cases} \quad (1)$$

where  $g$  is the average height of the watershed above the level of the draining system, in m;  $d$  is the maximum depth of acrotelm, in m;  $c$  is the bulk carbon density of peat, in  $\text{gC m}^{-3}$ ;  $A$  is the area of the grid cell in  $\text{m}^2$ ;  $f_{P,obs}$  is the fraction of the area occupied by peatlands; and  $h_{max}$  is the maximum height of water table above the level of draining system, in m.

The values of  $g$  at the cells of  $0.1^\circ \times 0.1^\circ$  geographic grid (Figure 1) were estimated from the data on depth to bedrock provided by SoilGrids (Hengl et al., 2014). The use of these data for estimating  $g$  in permafrost landscapes is somewhat challenging, because the hydraulic conductivity of permafrost could be as low as that of bedrock under some conditions. Due to this reason, we find it more suitable to use the maximum depth of the active layer for estimating  $g$  on these landscapes, for example, by setting  $g$  at 2 meters for the regions where mean annual temperature is below  $-2^\circ\text{C}$ , that is, assuming that the southern boundary of permafrost could be approximated by the  $-2^\circ\text{C}$  isotherm of mean annual temperature (Riseborough et al., 2008) and that the active layer thickness does not exceed 2 m. The latter is an *ad hoc* assumption based on the recent discussion of uncertainties in the methods for estimating active layer thickness at regional scale (Mishra et al., 2017).

To determine the present-day peatland extent, we relied on the WISE30sec data set (Batjes, 2016) of soil properties at  $30''$  resolution. The data set contains a classification of soil type for each mapping unit, and to diagnose peatland extent we determined the fraction of each  $0.1^\circ \times 0.1^\circ$  grid cell covered by soils of histosol type (soil code HS in FAO90 classification). These data allow us to estimate the values that  $f_P$  may take at the cells of the  $0.1^\circ \times 0.1^\circ$  geographic grid (Figure 2) and assume that peatlands occupy a total area of  $2.86 \times 10^6 \text{ km}^2$  in the land north of  $45^\circ\text{N}$ .

This estimate of the peatland area does not go beyond the recent estimates (Yu, 2012) (that fall in the range of 2-4 million  $\text{km}^2$ ), but it cannot be easily interpreted as the estimate of the actual peatland area. The estimates of the actual peatland area may vary depending on the criteria that are used to distinguish peatlands from other types of land surface. The minimal depth of the peat layer, which is used to classify a land unit as peatland, is the criterion that affects the estimates of peatland area. Since the data in soil properties do not allow us to evaluate the actual depth of peat layer, it would be better to interpret them as the area that could be potentially occupied by peatlands under the present climate.



Besides, the use of regular grid for representing the spatial distribution of peatland area imply large uncertainty in the estimate of  $p_{C,max}$  for a given cell. This problem could be illustrated with the following example. The fact that 36% of a grid cell is covered by peatlands may mean that peatlands cover 36% of each watershed within this grid cell (a conservative interpretation), or that only 48% of watersheds are occupied by peatlands, and they cover 75% ( $0.48 \times 75 = 36$ ) of each of these watersheds (a non-conservative interpretation).

Another illustration of the uncertainty associated with interpretation of  $f_{p,obs}$  is provided by Table 1, where the estimates of potential peat carbon density in the central part of peatlands are compared to the values observed at 33 peatland sites (Billings, 1987; Borren et al., 2004; Jones et al., 2009; Robinson, 2006; Turunen et al., 2001; Yu et al., 2009). As it can be seen from Table 1, the conservative estimates of the potential peat carbon density, that is, estimates based on the conservative interpretation of  $f_{p,obs}$ , are often lower than the actual peat carbon density at the sites that fall within the cells where  $f_{p,obs}$  is less than 20%.

The non-conservative interpretation of  $f_{p,obs}$  provides a much higher estimate of the potential carbon stocks in peatlands within latitudinal belt between  $45^\circ$  and  $84^\circ$  N than the conservative estimate: 1258 vs 665 PgC. This large uncertainty cannot be easily reduced by using a 1 km grid, because one cannot expect that each watershed falls within one grid cell. However, moving to finer grid is not the only approach for reducing uncertainty in the spatial distribution of peatlands. The value of the hydraulic conductivity coefficient,  $K$ , calculated from the amount of annual precipitation, potential evapotranspiration,  $f_{p,obs}$ , and  $g$  (see Supplement) could be used as an indicator of clustered peatland distribution within a grid cell. If it is above the typical value,  $K_c$ , then one may assume that peatland occupy  $f_{p,obs} / f_{p,est}$  fraction of watersheds and cover  $f_{p,est}$  fraction of area of each of these watersheds, where  $f_{p,est}$  is set at the value that brings  $K$  to  $K_c$ . Setting  $K_c$  at  $157 \text{ m yr}^{-1}$  ( $\approx 0.5 \times 10^{-5} \text{ m s}^{-1}$ ) leads to the estimate (Figure 3) that could be derived from the peat decomposition model that Yu (Yu, 2011) employed for estimating actual carbon stocks. This model suggests that the peat accumulation is limited by the ratio of peat C addition rate to the decay constant. Based on the data from peat cores, the peat C addition rate is estimated at  $74.8 \text{ TgC yr}^{-1}$  and decay constant at  $0.0000855 \text{ yr}^{-1}$  (Yu, 2011). Thus, the potential carbon stock in northern peatlands could be estimated at 875 PgC ( $74.8 / 0.0000855 = 874,853.8 \text{ TgC} \approx 875 \text{ PgC}$ ), and due to uncertainty in the peat C addition rate and decay constant may range from 750 to 1000 PgC (see Supplement).

### 3 Results

The results of our study suggest that even the conservative estimate of the potential carbon stocks (665 PgC) is still higher than Gorham's (1991) estimate of 455 PgC in the actual carbon stocks of northern peatlands. Gorham's estimate is the product of the four numbers: mean depth of peatlands (2.3 m), mean bulk density of peat ( $112 \times 10^3 \text{ g m}^{-3}$ ), carbon content of its dry mass (0.517), and the area of peatlands ( $3.42 \times 10^{12} \text{ m}^2$ ). Our conservative estimate of potential carbon stocks implies



that the potential mean depth of peat could be as high as 4 m for the same values of mean bulk density of peat and carbon content of its dry mass, and for smaller area of peatlands ( $2.86 \times 10^{12} \text{ m}^2$ ).

The conservative estimate is also higher than the Yu's (2011) estimate of actual carbon stocks,  $547 \pm 74 \text{ PgC}$ , based on the time history approach. However, it is lower than the estimate of the potential carbon stock of  $875 \pm 125 \text{ PgC}$  implied by the model of peat accumulation that Yu employed for estimating actual carbon stocks. This latter estimate of  $875 \pm 125 \text{ PgC}$  could be obtained under the less conservative interpretation of the data on soil properties (see *Methods*). The map of potential carbon density corresponding to this estimate is shown at Figure 3.

The highest estimate of the potential carbon stocks at  $1258 \text{ PgC}$  that could be obtained within the range of possible interpretations of the data on soil properties is beyond the range of uncertainty in the estimate of potential carbon stocks that could be derived using the Yu's model of peat accumulation, which ranges from 760 to  $1006 \text{ PgC}$ . Hence, one could find it reasonable to agree that the estimate of  $875 \pm 125 \text{ PgC}$ , as obtained from two completely independent methods, is the most expedient estimate of potential carbon stocks in northern peatlands.

#### 4 Discussion

The limits to northern peatlands carbon stock were estimated here for the first time in the literature, although the methodology for obtaining such estimate were developed more than 30 years ago by Clymo (1984). We adapted this methodology for use at the global scale and for taking into account geomorphological aspects of peat bog growth represented by the gridded data on the depth to bedrock (Hengl et al., 2014).

Moreover, this estimate corresponds to the present climate, and therefore assumes that the present climate is somewhat typical for the present interglacial period. This assumption, perhaps, is not relevant to the scenarios of dramatic changes in the Earth system that might take place if cumulative carbon emissions exceed  $1000 \text{ PgC}$ . But if cumulative carbon emissions would not exceed  $1000 \text{ PgC}$ , the northern peatlands would play an important role in global carbon cycle recovery.

The ultimate recovery of the global carbon cycle from anthropogenic emissions is a long-term process. The current understanding of this process suggests that oceans absorb the majority of cumulative carbon dioxide emission within several centuries, the minor portion within several thousand years, and the remaining part will be removed through weathering of silicate rocks that may take hundreds of thousands of years (Archer, 2005; Archer and Brovkin, 2008; Brault et al., 2017). In plain words, the larger the perturbation of the Earth system, the lower the chances that the pre-industrial state will be restored in course of the current interglacial.

Including peatlands in the consideration of global carbon cycle recovery allows us to evaluate the level of the Earth system perturbation that would not last too long to "break" the glacial-interglacial cycle. The results of numerical experiments (see Supplement) performed using an Earth system model of intermediate complexity (Brovkin et al., 2016) imply that keeping



cumulative carbon dioxide emissions below 1000 PgC essentially reduces the risk of human intervention of natural glacial-interglacial cycle (Figure 4). The northern peatlands are capable to remove in relevant time frame the amount of carbon that ocean won't remove, and thus to reduce the atmospheric carbon dioxide concentration to the level that is typical of interglacial periods.

## 5 Conclusions

Northern peatlands accumulate organic carbon and serve as a slow but persistent land carbon sink since the beginning of the current interglacial. If there were no limits to their growth in the absence of anthropogenic or natural CO<sub>2</sub> sources to the atmosphere, they could eventually reduce the atmospheric carbon dioxide concentration to the level at which a next precession-driven decline in the summer insolation in the high northern latitudes would trigger the onset of glaciation.

- 10 Our study, however, shows that the cumulative carbon removal associated with the natural development of peatland ecosystems is limited. The most expedient estimate of its potential magnitude,  $875 \pm 125$  PgC, was obtained under assumption that the present climate is somewhat typical for the current interglacial period. Unless future scenarios of changes in the Earth system would leave no room for northern peatlands, the northern peatlands will play an important role in global carbon cycle recovery from anthropogenic emissions. While studies of this process are now focused on the strength and capacity of
- 15 the ocean carbon sink, our results open a new perspective for the research on global carbon cycle recovery and on the measures needed to protect the northern peatlands as an important element of the Earth's climate system.

**Data availability.** All data used in this study are available from public databases or literature, cited in the Methods section. The data produced in course of this work are available from Georgii Alexandrov ([g.alexandrov@ifaran.ru](mailto:g.alexandrov@ifaran.ru)) upon request.

20

**Author Contributions.** All authors contributed to the conception of the work, to data processing and to writing of the paper. G.A.A. drafted the manuscript with inputs from V.A.B., T.K., and Z.Y.

**Competing interests.** The Authors declare no conflict of interests.

25

**Acknowledgements.** G.A.A. acknowledges funding by RFBR according to the research project № 19-05-00534. The manuscript has been initiated during a visit of G.A.A. to the Land in the Earth System Department of the Max Planck Institute of Meteorology in 2017.



## References

- Adams, J. M. and Faure, H.: A new estimate of changing carbon storage on land since the last glacial maximum, based on global land ecosystem reconstruction, *Glob. Planet. Change*, 16–17, 3–24, doi:10.1016/S0921-8181(98)00003-4, 1998.
- Alexandrov, G. A., Brovkin, V. A. and Kleinen, T.: The influence of climate on peatland extent in Western Siberia since the  
5 Last Glacial Maximum, *Sci. Rep.*, 6, doi:10.1038/srep24784, 2016.
- Archer, D.: Fate of fossil fuel CO<sub>2</sub> in geologic time, *J. Geophys. Res. C Ocean.*, 110(9), 1–6, doi:10.1029/2004JC002625, 2005.
- Archer, D. and Brovkin, V.: The millennial atmospheric lifetime of anthropogenic CO<sub>2</sub>, *Clim. Change*, 90(3), 283–297, doi:10.1007/s10584-008-9413-1, 2008.
- 10 Batjes, N. H.: Harmonized soil property values for broad-scale modelling (WISE30sec) with estimates of global soil carbon stocks, *Geoderma*, 269, 61–68, doi:10.1016/j.geoderma.2016.01.034, 2016.
- Berger, B., Crucifix, M., Hodell, D. A., Mangili, C., McManus, J. F., Otto-Bliesner, B., Pol, K., Raynaud, D., Skinner, L. C., Tzedakis, P. C., Wolff, E. W., Yin, Q. Z., Abe-Ouchi, A., Barbante, C., Brovkin, V., Cacho, I., Capron, E., Ferretti, P., Ganopolski, A., Grimalt, J. O., Hoffmann, B., Kawamura, K. A., Landais, A., Margari, V., Martrat, B., Masson-Delmotte, V.,  
15 Mokeddem, Z., Parrenin, F., Prokopenko, A. A., Rashid, H., Schulz, M. and Vazquez Riveiros, N.: Interglacials of the last 800,000 years, *Rev. Geophys.*, 54(1), 162–219, doi:10.1002/2015RG000482, 2016.
- Billings, W. D.: Carbon balance of Alaskan tundra and taiga ecosystems: past, present and future, *Quat. Sci. Rev.*, 6(2), 165–177, doi:10.1016/0277-3791(87)90032-1, 1987.
- Borren, W., Bleuten, W. and Lapshina, E. D.: Holocene peat and carbon accumulation rates in the southern taiga of western  
20 Siberia, *Quat. Res.*, 61(1), 42–51, doi:10.1016/j.yqres.2003.09.002, 2004.
- Brault, M.-O., Matthews, H. D. and Mysak, L. A.: The importance of terrestrial weathering changes in multimillennial recovery of the global carbon cycle: a two-dimensional perspective, *Earth Syst. Dyn. Discuss.*, (January), 1–65, doi:10.5194/esd-2016-53, 2017.
- Brovkin, V., Brücher, T., Kleinen, T., Zaehle, S., Joos, F., Roth, R., Spahni, R., Schmitt, J., Fischer, H., Leuenberger, M.,  
25 Stone, E. J., Ridgwell, A., Chappellaz, J., Kehrwald, N., Barbante, C., Blunier, T. and Dahl Jensen, D.: Comparative carbon cycle dynamics of the present and last interglacial, *Quat. Sci. Rev.*, 137, 15–32, doi:10.1016/j.quascirev.2016.01.028, 2016.
- Clymo, R. S.: The Limits to Peat Bog Growth, *Philos. Trans. R. Soc. B Biol. Sci.*, 303(1117), 605–654, doi:10.1098/rstb.1984.0002, 1984.
- Gorham, E.: Northern peatlands: role in the carbon cycle and probable responses to climatic warming, *Ecol. Appl.*, 1(2),



- 182–195, doi:10.2307/1941811, 1991.
- Hengl, T., de Jesus, J. M., MacMillan, R. A., Batjes, N. H., Heuvelink, G. B. M., Ribeiro, E., Samuel-Rosa, A., Kempen, B., Leenaars, J. G. B., Walsh, M. G. and Gonzalez, M. R.: SoilGrids1km — Global Soil Information Based on Automated Mapping, *PLoS One*, 9(8), e105992, doi:10.1371/journal.pone.0105992, 2014.
- 5 Jones, M. C., Peteet, D. M., Kurdyla, D. and Guilderson, T.: Climate and vegetation history from a 14,000-year peatland record, Kenai Peninsula, Alaska, *Quat. Res.*, 72(2), 207–217, doi:10.1016/j.yqres.2009.04.002, 2009.
- Loisel, J., Yu, Z., Beilman, D. W., Camill, P., Alm, J., Amesbury, M. J., Anderson, D., Andersson, S., Bochicchio, C., Barber, K., Belyea, L. R., Bunbury, J., Chambers, F. M., Charman, D. J., De Vleeschouwer, F., Fiałkiewicz-Kozieł, B., Finkelstein, S. A., Gałka, M., Garneau, M., Hammarlund, D., Hinchcliffe, W., Holmquist, J., Hughes, P., Jones, M. C.,
- 10 Klein, E. S., Kokfelt, U., Korhola, A., Kuhry, P., Lamarre, A., Lamentowicz, M., Large, D., Lavoie, M., MacDonald, G., Magnan, G., Mäkilä, M., Mallon, G., Mathijssen, P., Mauquoy, D., McCarroll, J., Moore, T. R., Nichols, J., O'Reilly, B., Oksanen, P., Packalen, M., Peteet, D., Richard, P. J. H., Robinson, S., Ronkainen, T., Rundgren, M., Sannel, A. B. K., Tarnocai, C., Thom, T., Tuittila, E. S., Turetsky, M., Väliranta, M., van der Linden, M., van Geel, B., van Bellen, S., Vitt, D., Zhao, Y. and Zhou, W.: A database and synthesis of northern peatland soil properties and Holocene carbon and nitrogen
- 15 accumulation, *Holocene*, doi:10.1177/0959683614538073, 2014.
- Loisel, J., van Bellen, S., Pelletier, L., Talbot, J., Hugelius, G., Karran, D., Yu, Z., Nichols, J. and Holmquist, J.: Insights and issues with estimating northern peatland carbon stocks and fluxes since the Last Glacial Maximum, *Earth-Science Rev.*, doi:10.1016/j.earscirev.2016.12.001, 2017.
- Mishra, U., Drewniak, B., Jastrow, J. D., Matamala, R. M. and Vitharana, U. W. A.: Spatial representation of organic carbon and active-layer thickness of high latitude soils in CMIP5 earth system models, *Geoderma*, 300, 55–63, doi:10.1016/j.geoderma.2016.04.017, 2017.
- Raupach, M. R., Davis, S. J., Peters, G. P., Andrew, R. M., Canadell, J. G., Ciais, P., Friedlingstein, P., Jotzo, F., van Vuuren, D. P. and Le Quéré, C.: Sharing a quota on cumulative carbon emissions, *Nat. Clim. Chang.*, 4(10), 873–879, doi:10.1038/nclimate2384, 2014.
- 25 Riseborough, D., Shiklomanov, N., Etzelmüller, B., Gruber, S. and Marchenko, S.: Recent advances in permafrost modelling, *Permafr. Periglac. Process.*, 19(2), 137–156, doi:10.1002/ppp.615, 2008.
- Robinson, S. D.: Carbon accumulation in peatlands, southwestern Northwest Territories, Canada, *Can. J. Soil Sci.*, 86(Special Issue), 305–319, doi:10.4141/S05-086, 2006.
- Turunen, J., Tahvanainen, T., Tolonen, K. and Pitkänen, A.: Carbon accumulation in West Siberian mires, Russia, *Global*
- 30 *Biogeochem. Cycles*, 15(2), 285–296, doi:10.1029/2000GB001312, 2001.



Yu, Z.: Holocene carbon flux histories of the world's peatlands: Global carbon-cycle implications, *The Holocene*, 21(5), 761–774, doi:10.1177/0959683610386982, 2011.

Yu, Z., Beilman, D. W. and Jones, M. C.: Sensitivity of Northern Peatland Carbon Dynamics to Holocene Climate Change, in *Carbon Cycling in Northern Peatlands*, pp. 55–69., 2009.

- 5 Yu, Z., Loisel, J., Brosseau, D. P., Beilman, D. W. and Hunt, S. J.: Global peatland dynamics since the Last Glacial Maximum, *Geophys. Res. Lett.*, 37(13), doi:10.1029/2010GL043584, 2010.

Yu, Z. C.: Northern peatland carbon stocks and dynamics: A review, *Biogeosciences*, 9(10), 4071–4085, doi:10.5194/bg-9-4071-2012, 2012.



**Table 1. Potential peat carbon density at the central part of peatland estimated under conservative (PCD1) and non-conservative (PCD2) interpretation of  $f_{p, obs}$  as compared to the observed peat carbon density (PCD0) at 33 peatland sites (Yu et al., 2009).**

| Site # | Region       | Type       | Location         | PCD0<br>kgC m <sup>-2</sup> | PCD1<br>kgC m <sup>-2</sup> | PCD2<br>kgC m <sup>-2</sup> | $f_{p, obs}$<br>% |
|--------|--------------|------------|------------------|-----------------------------|-----------------------------|-----------------------------|-------------------|
| 1      | West Siberia | bog        | 60°10'N 72°50'E  | 230                         | 1148                        | 2239                        | 56                |
| 2      | West Siberia | bog        | 60°10'N 72°50'E  | 268                         | 1148                        | 2239                        | 56                |
| 3      | West Siberia | bog        | 56°50'N 78°25'E  | 413                         | 1277                        | 1432                        | 72                |
| 4      | West Siberia | fen        | 56°20'N 84°35'E  | 399                         | 849                         | 1444                        | 60                |
| 5      | Alaska       | fen        | 60°27'N 151°14'W | 149                         | 190                         | 1437                        | 20                |
| 6      | Alaska       | fen        | 60°38'N 151°04'W | 142                         | 191                         | 1449                        | 20                |
| 7      | Alaska       | rich fen   | 60°25'N 150°54'W | 117                         | 157                         | 1155                        | 20                |
| 8      | Alaska       | poor fen   | 60°47'N 150°49'W | 64                          | 219                         | 1687                        | 20                |
| 9      | Alaska       | taiga bog  | 64°52'N 147°46'W | 133                         | 102                         | 692                         | 20                |
| 10     | Canada       | slope bog  | 54°09'N 130°15'W | 73                          | N/A                         | N/A                         | 0                 |
| 11     | Canada       | rich fen   | 53°35'N 118°01'W | 232                         | 68                          | 864                         | 10                |
| 12     | Canada       | fen        | 52°27'N 116°12'W | 317                         | 55                          | 623                         | 10                |
| 13     | Canada       | bog        | 55°01'N 114°09'W | 228                         | 1499                        | 1811                        | 70                |
| 14     | Canada       | permafrost | 61°48'N 121°24'W | 147                         | 72                          | 566                         | 16                |
| 15     | Canada       | fen        | 68°17'N 133°15'W | 61                          | 82                          | 524                         | 20                |
| 16     | Canada       | fen        | 69°29'N 132°40'W | 27                          | N/A                         | N/A                         | 0                 |
| 17     | Canada       | permafrost | 55°51'N 107°41'W | 141                         | 99                          | 1294                        | 11                |
| 18     | Canada       | fen        | 64°43'N 105°34'W | 65                          | N/A                         | N/A                         | 0                 |
| 19     | Canada       | fen        | 66°27'N 104°50'W | 84                          | N/A                         | N/A                         | 0                 |
| 20     | Canada       | permafrost | 59°53'N 104°12'W | 81                          | N/A                         | N/A                         | 0                 |
| 21     | Canada       | bog        | 45°41'N 74°02'W  | 70                          | N/A                         | N/A                         | 0                 |
| 22     | Canada       | rich fen   | 82°N 68°W        | 97                          | N/A                         | N/A                         | 0                 |
| 23     | Canada       | N/A        | 47°56'N 64°30'W  | 275                         | 58                          | 678                         | 10                |
| 24     | Canada       | N/A        | 45°56'N 60°16'W  | 209                         | 54                          | 606                         | 10                |
| 25     | Scotland     | bog        | 57°31'N 5°09'W   | 106                         | N/A                         | N/A                         | 0                 |
| 26     | Scotland     | bog        | 57°34'N 5°22'W   | 195                         | 129                         | 873                         | 21                |
| 27     | Scotland     | bog        | 57°41'N 5°41'W   | 151                         | 160                         | 493                         | 40                |
| 28     | Finland      | palsa mire | 68°24'N 23°33'E  | 122                         | 190                         | 1438                        | 20                |
| 29     | Finland      | fen        | 68°24'N 23°33'E  | 134                         | 190                         | 1438                        | 20                |
| 30     | Finland      | raised bog | 60°49'N 26°57'E  | 214                         | 65                          | 1350                        | 6                 |
| 31     | Finland      | aapa mire  | 65°39'N 27°19'E  | 123                         | 499                         | 994                         | 55                |
| 32     | Finland      | aapa mire  | 65°39'N 27°19'E  | 154                         | 499                         | 994                         | 55                |
| 33     | Finland      | fen        | 65°39'N 27°19'E  | 215                         | 499                         | 994                         | 55                |

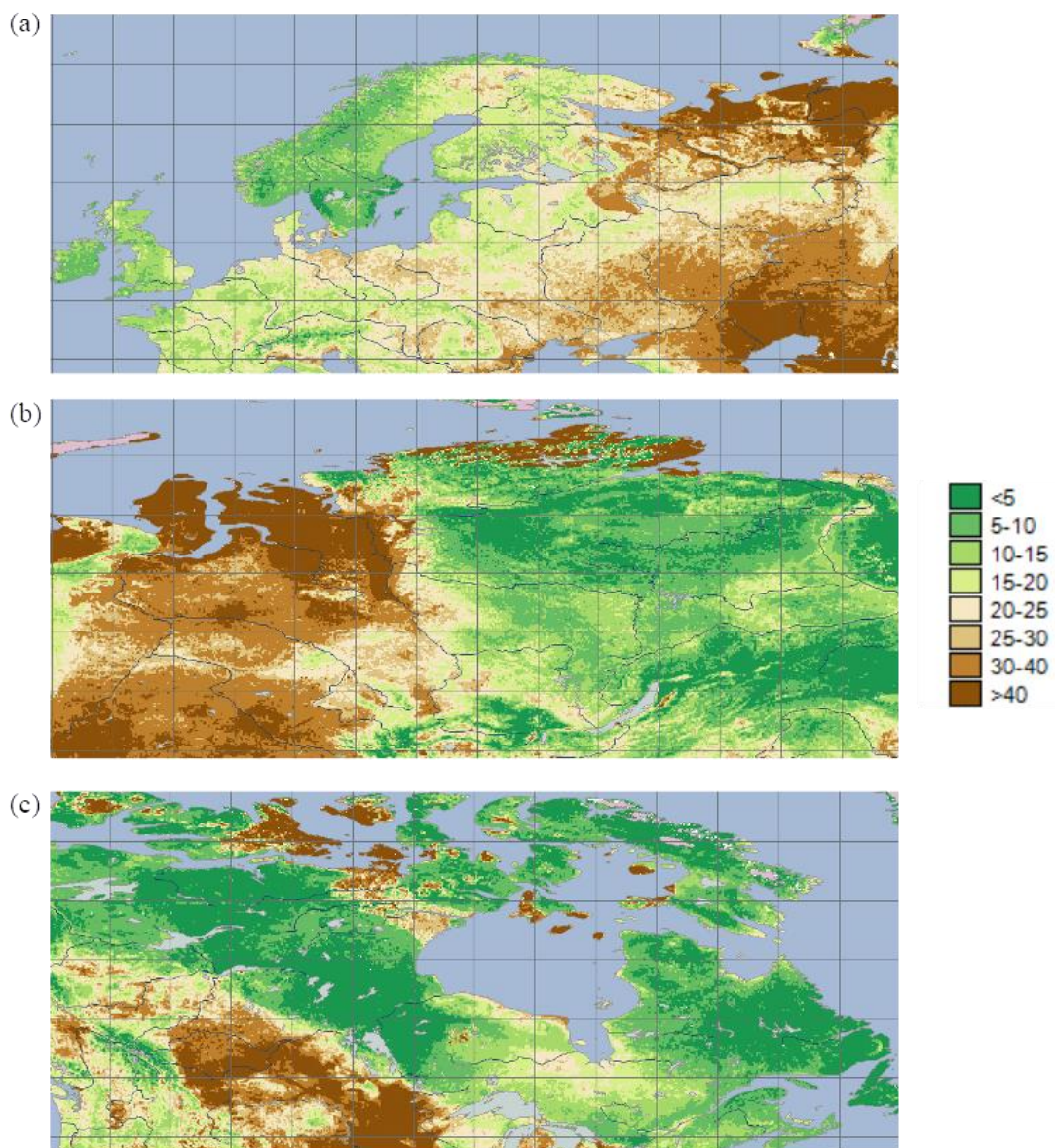
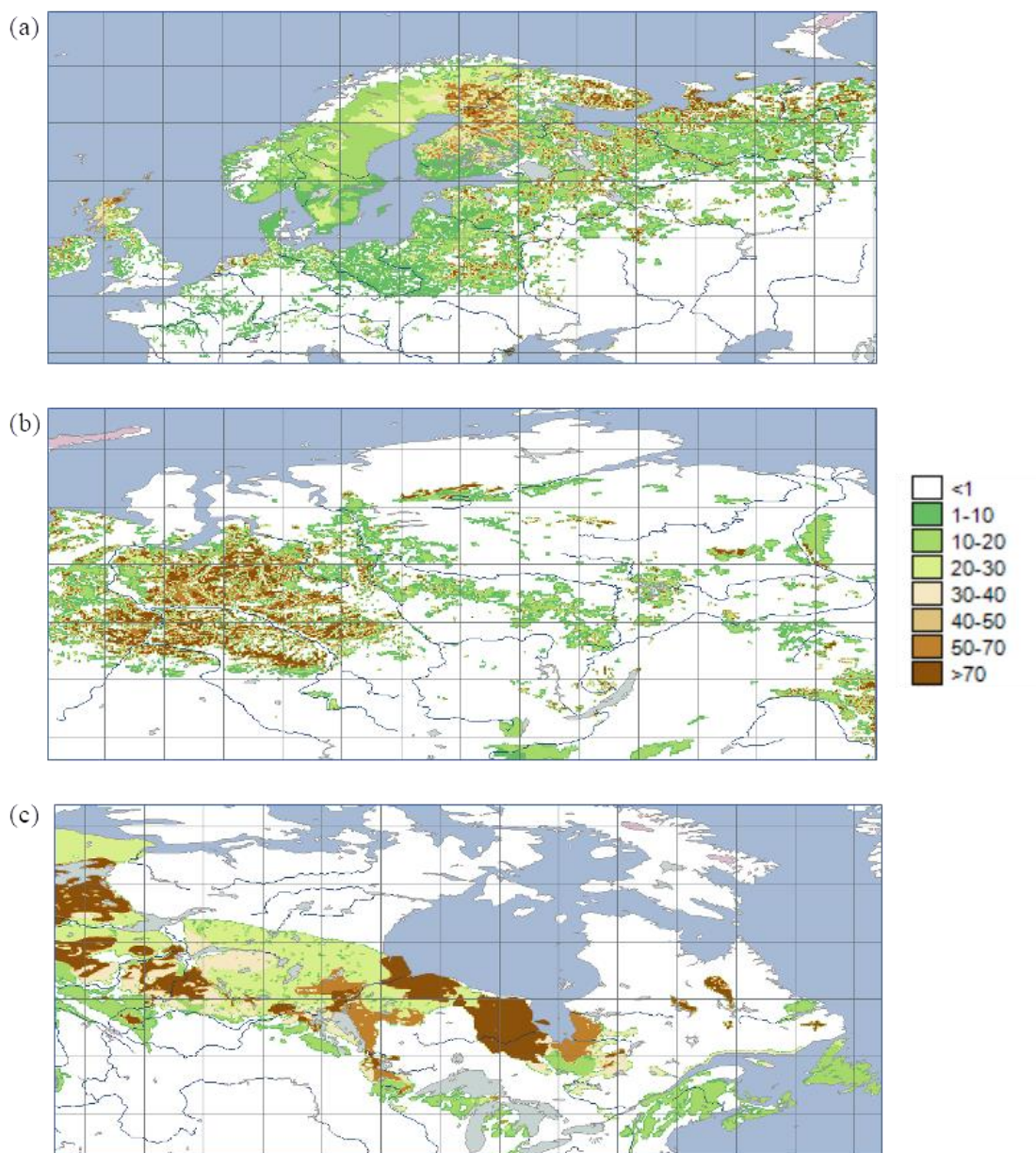
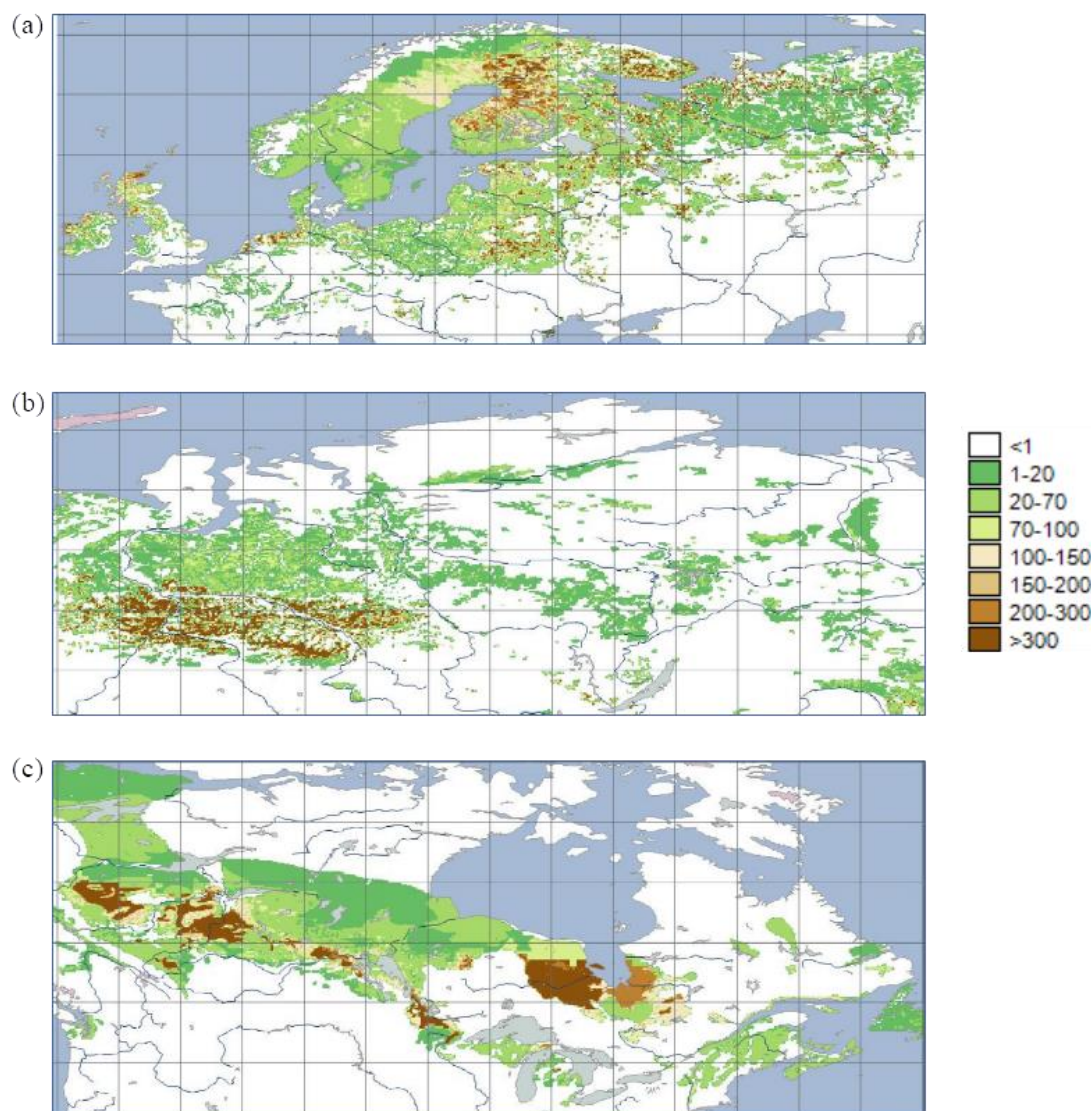


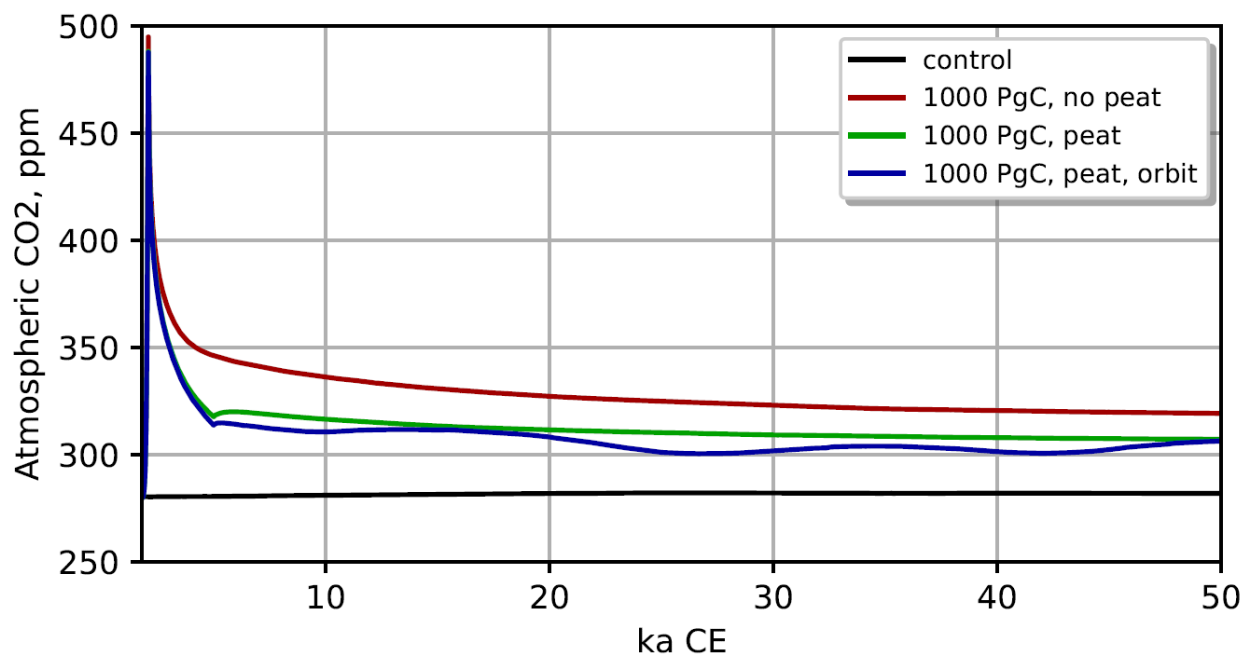
Figure 1: The depth to bedrock, an estimate of  $g$ , in meters, in Europe (a), Western Siberia (b), Canada (c).



**Figure 2: The fraction of histosols (%) in Europe (a), Western Siberia (b), and Canada (c).**



**Figure 3:** The less-conservative estimate of the potential carbon stocks in northern peatlands per area of a grid cell ( $\times 10^9$  gC km<sup>-2</sup>) in Europe (a), Western Siberia (b), and Canada (c).



5 Figure 4: Multimillennial changes in the atmospheric CO<sub>2</sub> concentration simulated using CLIMBER-2, an Earth system model of intermediate complexity (Brovkin et al., 2016), for scenario of 1000 PgC cumulative emissions. No peatlands (mainly ocean CO<sub>2</sub> uptake, red line), plus northern peatlands uptake of 330 PgC (green line), plus orbital forcing effect (blue line).